Wave overtopping discharges at rubble mound breakwaters including effects of a crest wall and a berm

van Gent, Marcel R.A.; Wolters, Guido; Capel, Alex

Wave overtopping discharges at rubble mound breakwaters including effects of a crest wall and a berm

Marcel R.A. van Gent [a,b,*], Guido Wolters [a], Alex Capel [a]

[a] Dept. Coastal Structures & Waves, Deltares, Delft, the Netherlands
[b] Dept. Hydraulic Engineering, TU Delft, Delft, the Netherlands

ARTICLE INFO

ABSTRACT

Physical model tests have been performed to study wave overtopping at rubble mound breakwaters, including breakwaters with a crest wall, breakwaters with a berm, and breakwaters with a crest wall and a berm. For rubble mound structures with a protruding crest wall or with a stable berm, limited information is available in literature even though protruding crest walls and berms clearly affect wave overtopping discharges. Adding a crest wall to an existing structure, increasing the height of a crest wall, adding a berm, or increasing the width or height of a berm, can be effective measures to account for effects of sea level rise if the sea level rise appears to be more severe than the amount of sea level rise for which the structure was designed for. The present wave flume tests were used to develop guidelines for rubble mound breakwaters, including breakwaters with a crest wall or with a berm. The relative height of the protruding part of a crest wall dominates the effect of a crest wall. The berm width, berm level and wave steepness all affect the influence of a berm on the wave overtopping discharge. Moreover, it was confirmed that the wave steepness also affects wave overtopping discharges for rubble mound breakwaters without a berm or without a crest wall. The developed set of expressions for rubble mound structures has also been validated based on existing data for oblique wave attack on rubble mound breakwaters with a crest wall.

1. Introduction

For the design and adaptation of coastal structures, accurate wave overtopping estimates are important to meet the functional requirements of the structures. Adaptation of existing coastal structures has become more important due to climate change and the resulting sea level rise. Especially for coastal structures that are in relatively shallow water, sea level rise can cause an increase in wave loading on the coastal structure since less dissipation of wave energy occurs before the waves reach the structure. Estimates of the speed of sea level rise are changing and uncertain. Therefore, it may be suitable to design coastal structures that can be adapted once the sea level rise appears to be more severe than expected.

Other adaptation measures than an increase of the crest level can be considered, such as dissipating energy before waves reach the structure (by increasing the foreshore by sand nourishment to dissipate more wave energy, or by constructing a low-crested structure in front of existing structures), increasing the dissipation on the structure (by applying a berm in the seaward slope or by increase the roughness of the slope of a dike), modifying the crest (by for instance applying or modifying a crest element), or increasing the resistance to wave overtopping at the crest and rear side of the structure (see also Fig. 1). Such adaptations require accurate prediction methods to estimate wave overtopping (denoted by a discharge q). Especially for the combination of two or more of such adaptation measures, the validity of available design guidelines on wave overtopping is unknown or they do not provide suitable guidance at all (see for instance Van Gent, 2019, and Hogeveen, 2021).

Hogeveen (2021) studied climate adaptation of rubble mound breakwaters by using climate adaption pathways and analysed the costs of adaptation measures and pathways. Fig. 2 shows an example of an adaptation pathway map, where on the vertical the adaptation measures are shown and on the horizontal axis the sea level rise is shown. Each adaptation measure has a limit to the amount of sea level rise that it can compensate for (i.e. tipping points: vertical bold black lines in Fig. 2). For instance, if an increased foreshore is required to stay below water during daily conditions this limits the effectiveness. Or, if the strength of a crest wall limits the height of the protruding part of the crest wall, this

limits the applicability of a protruding crest wall. The costs for each pathway (*i.e.* each combination of adaptation measures such as first adding a berm and thereafter adding a protruding crest wall) can be calculated to determine the most economical combination of adaptation measures. For severe sea level rise scenarios, a combination of adaptation measures may be required. Hogeveen (2021) concluded that adding a berm to a rubble mound structure and adding a protruding crest wall can be economically attractive if existing structures need to be adapted due to the consequences of sea level rise.

For statically stable (*i.e.* non-reshaping) rubble mound breakwaters available manuals do hardly provide information on the effects of a berm or the effects of a protruding crest element. For instance, in the expression proposed in EurOtop (2018; Eq. (6.5)) the berm does not affect wave overtopping discharges for rubble mound structures and no guidance is provided for the effect of protruding crest walls. Nevertheless, both berms and protruding crest walls are frequently being applied in practice since they appear to be effective and economically attractive. Also, numerical modelling such as performed by Hogeveen (2021) and applying machine learning methods based on data from physical model tests such as performed by Van Gent et al. (2007), Molines and Medina (2016), and Den Bieman et al. (2021) indicate that a berm or a crest wall affect wave overtopping discharges. Besides numerical models and machine learning techniques that are capable of computing wave overtopping discharges, it is also desirable to have easy-to-apply empirical expressions available to estimate wave overtopping discharges, including expressions that account for a berm in the seaward slope and for a crest wall. The mentioned methods based on machine learning are also easy to apply but the data sets on which they are based contain a relatively small amount of data for rubble mound structures that contain both a berm and a crest wall. In the present study physical model tests are used to develop empirical expressions to estimate wave overtopping discharges at rubble mound breakwaters, including breakwaters with a berm, breakwaters with a crest wall, and breakwaters with a combination of both.

The structure of the paper is as follows. In Section 2 a selection of literature on wave overtopping is discussed. In Section 3 the physical model tests are described. In Section 4 new empirical expressions are presented and discussed. Section 5 provides conclusions and recommendations.

2. Wave overtopping

Wave overtopping at coastal structures can be characterised by mean overtopping discharges during the peak of a storm, by overtopping volumes per wave, and by flow velocities and the flow depth during wave overtopping events. Koosheh et al. (2021) provides an overview of knowledge with respect to overtopping volumes per wave. See also Mares-Nasarre et al. (2020) for a recent study on overtopping volumes at rubble mound breakwaters. For estimates of flow velocities and the flow depth during wave overtopping events reference is made to Schüttrumpf (2001), Van Gent (2001, 2002b), Schüttrumpf and Van Gent (2003), Van Bergeijk et al. (2019), and Mares-Nasarre et al. (2021).

The present study is focussed on mean overtopping discharges at rubble mound breakwaters. It is important to realise that the mean overtopping discharge may not be the only wave overtopping parameter that is of importance. For instance, for the same mean overtopping discharge the horizontal velocities of the water that overtops the breakwater may be significantly lower for a breakwater with a vertical protruding crest wall than for a rubble mound breakwater without a vertical protruding element. The reduction in horizontal velocities due to the crest wall may reduce the risk for activities and facilities behind the crest, which is not fully expressed by using the mean overtopping discharge as the parameter to describe wave overtopping.

Goda (1971), Battjes (1974) and Owen (1980) performed pioneering research with respect to wave overtopping. After that, various formulas have been developed to predict wave overtopping at rubble mound breakwaters of which many can be rewritten as follows:

$$\frac{q}{\sqrt{gH_{m0}^3}} = a \, \exp\left[-\frac{b}{\gamma} \, \left(\frac{R_c}{H_{m0}} \right)^c \right] \tag{1}$$

where q is the mean wave overtopping discharge (m³/s/m), g is the acceleration due to gravity (m/s²), R_c is the freeboard (including the height of a crest wall, if present) relative to the still water level (m), H_{m0} ($H_{m0} = 4\sqrt{m_0}$) is the spectral significant wave height of the incident waves at the toe of the structure $H_s = H_{m0}$ (m), and γ denotes the influence factor (−) for effects such as the influence of roughness (γ_f) and the influence of oblique waves (γ_β); a and b and c are coefficients. For the coefficient c TAW (2002) uses $c = 1$, EurOtop (2018) uses $c = 1.3$, while Gallach-Sánchez (2018) and Gallach-Sánchez et al. (2021) calibrated the coefficient c based on extensive tests and proposed the value $c = 1.1$. Note that $Q = q/(gH_{m0}^3)^{0.5}$ is the non-dimensional wave overtopping discharge.

Some manuals (*e.g.* TAW, 2002) provide different expressions for plunging waves (also called "breaking waves") and for surging waves (also called "non-breaking waves") for wave run-up and wave overtopping. The expressions for surging waves serve as an upper limit for estimates obtained using the expressions for plunging waves. Whereas coastal structures with a gentle seaward slope such as dikes often result in the expressions for plunging waves ("breaking waves") being used, structures with steeper slopes such as rubble mound breakwaters lead to expressions for surging waves ("non-breaking waves") being used (*i.e.* Eq. (1)), especially for the design conditions. Existing expressions for plunging waves contain an influence of the slope of the structure, the wave steepness, a berm (if present), a crest wall (if present) and other influence factors. However, the expression for surging waves, *i.e.* Eq. (1), describes no influence of the slope of the structure, no influence of the wave steepness, no influence of a berm (if present), and no influence of a crest wall (if present) on the wave overtopping discharges. Despite that the expressions for surging waves on dikes or on rubble mound
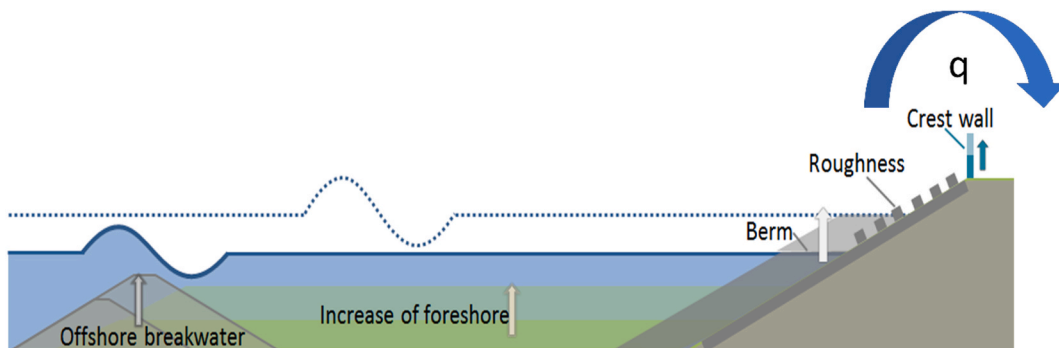

Fig. 1. Adaptation measures for existing coastal structures.

breakwaters (in for instance TAW, 2002, Eq. (23), and EurOtop, 2018, Eq. (6.5)) predict no influence of the wave steepness, a berm or a crest wall, the present study on statically stable (*i.e.* non-reshaping) rubble mound breakwaters is focussed on the influence of these.

Lioutas et al. (2012) and Koosheh et al. (2022) showed that for rock armoured revetments with an impermeable core the wave steepness affects the mean overtopping discharge. Koosheh et al. (2022) proposed the following expression:

$$\frac{q}{\sqrt{gH_{m0}^3}} = a \ \exp\left[-\frac{b}{\gamma} \ \left(\frac{R_c}{H_{m0}} \right)^c s_{m-1,0}^d \right] \qquad (2)$$

where $a = 0.05$, $b = 4.52$, $c = 1.12$, $d = 0.35$ and the wave steepness $s_{m-1,0} = 2\pi \ H_{m0}/gT_{m-1,0}^2$ is based on the significant wave height of the incident waves at the toe of the structure $H_s = H_{m0}$ (m) and the mean spectral wave period $T_{m-1,0}$ (s). As shown in Van Gent (1999, 2001, 2002a) the spectral wave period $T_{m-1,0}$ ($T_{m-1,0} = m_{-1}/m_0$) is the most suitable wave period to account for the influence of the spectral shape on wave run-up and wave overtopping.

Sigurdarson and van der Meer (2012) studied wave overtopping at (reshaping) berm breakwaters. The reshaping of berm breakwaters can cause that the overtopping characteristics change depending on the reshaping. However, they also examined partly and hardly reshaping berm breakwaters and concluded that the overtopping depends on the wave steepness (based on the peak wave period) and the berm width B (see also Fig. 3). The effects of the wave steepness and the berm width were accounted for by a modified expression for the influence factor γ_f for roughness for partly and hardly reshaping berm breakwaters, that was rewritten in EurOtop (2018, Eq. (6.11)) to apply the spectral wave period instead of the peak wave period: $\gamma_f = \gamma_{BB} = 0.68 - 4.1s_{m-1,0} - 0.05B/H_s$. Although the present study is focussed on statically stable rubble mound breakwaters and not on reshaping berm breakwaters, this provides an indication that the berm and wave steepness affect wave overtopping also for non-reshaping rubble mound breakwaters. Also, Christensen et al. (2014) found a dependency of the wave overtopping discharge on the wave steepness. Additional information on the influence of parameters on wave overtopping at reshaping berm breakwaters can be found in Pillai et al. (2017a,b).

2.1. Crest wall influence

For the influence of a crest wall on wave overtopping at impermeable dikes, detailed information is available (Van Doorslaer, 2018). For impermeable structures a crest wall leads to a reduction in wave overtopping compared to an impermeable structure without a crest wall but with the same total crest elevation (*i.e.* same R_c). For rubble mound breakwaters the influence of a crest wall can be significantly different than for impermeable dikes. The roughness and permeability of the armour layer can be more effective in reducing the wave overtopping discharge than a crest wall. Therefore, the expressions derived by Van Doorslaer (2018) cannot be used, since the influence of a crest wall is generally a reducing effect for dikes, while for rubble mound breakwaters the application of a crest wall can increase the discharge for structures with the same crest elevation. Obviously, adding a protruding crest wall to an existing structure leading to an increased crest elevation R_c, reduces the discharge.

Since there are clear indications that a crest wall affects wave overtopping not only for gentle sloped structures such as dikes, but also for (steep) rubble mound breakwaters, an empirical expression to account for the effects of a crest wall is required. Adding a crest wall with a recurved parapet (or bullnose) to an existing structure can potentially reduce the wave overtopping. However, the present study is focused on crest walls without a recurved parapet.

2.2. Berm influence

For the influence of berms in the seaward slope, detailed information is available for impermeable slopes such as for dikes; reference is made to De Waal and van der Meer (1992), Chen et al. (2020), and Van Gent (2020). For the influence of berms on wave overtopping at rubble mound breakwaters less information is available; reference is made to Krom (2012). Note that here breakwaters with a statically stable berm are dealt with and not berm breakwaters for which the berm is allowed to reshape to some extent. Since there are clear indications that the berm affects wave overtopping not only for gentle sloped impermeable structures, but also for rubble mound breakwaters, an empirical expression to account for the effects of a berm is required. The present study is focussed on rubble mound breakwaters with a horizontal berm (with a width B and tan $\alpha_B = 0$, see Fig. 3).

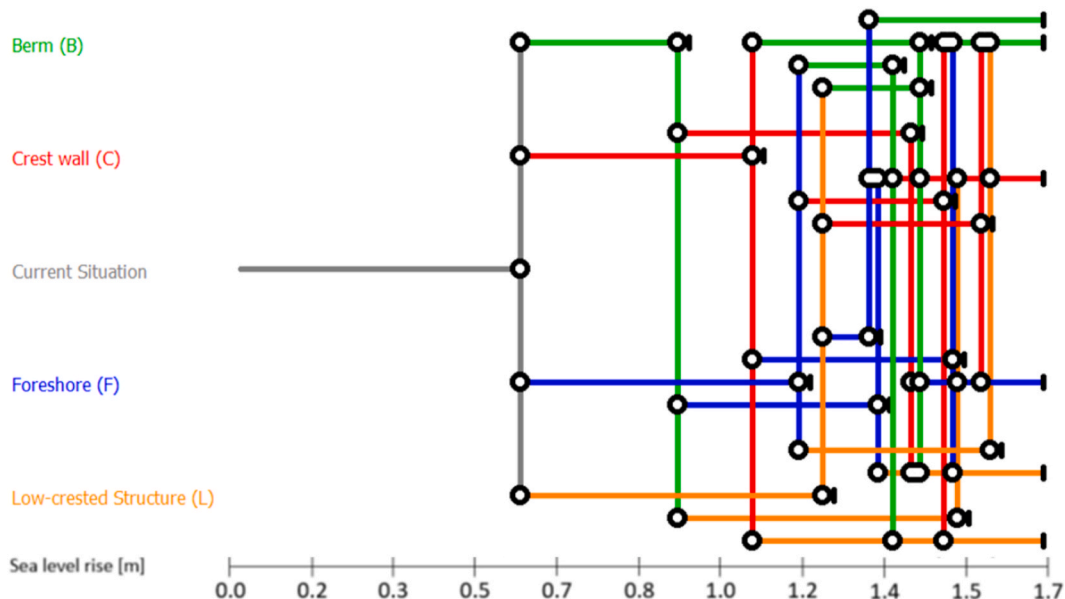Adapting an existing rubble mound breakwater is feasible by adding

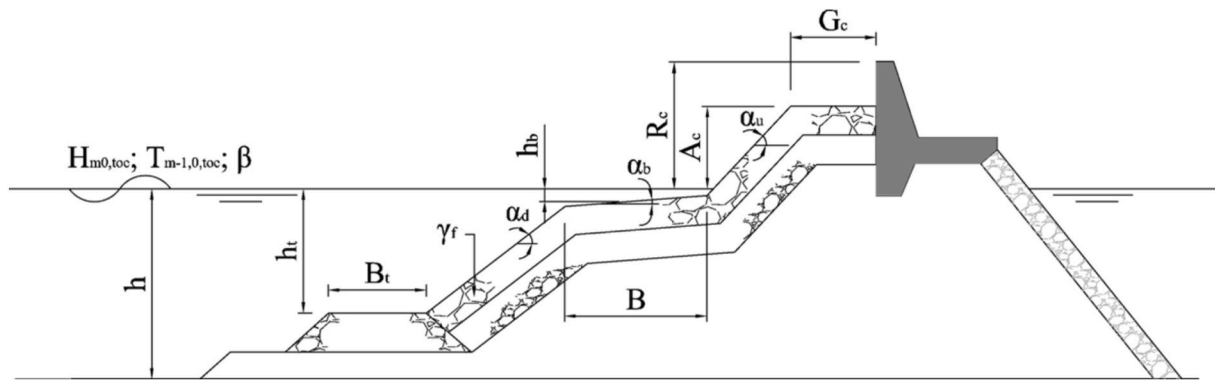**Fig. 2.** Adaptation pathways for a rubble mound breakwater (from: Hogeveen, 2021).

Fig. 3. Definition of parameters (figure from Van Gent et al., 2007).

a berm in front of the armour layer. Obviously, for structures that are in relatively shallow water, the required amount of material is less than for structures in deeper water. For structures that already have a berm, effects of sea level rise on wave overtopping discharges may be reduced by increasing the level of the berm such that the berm becomes more effective.

Besides that separate methods to account for the effect of a berm and a crest wall on wave overtopping discharges are required, these methods need to be validated for structures that have both a berm and a crest wall. Therefore, the tests described in the following section also contain a large number of tests with structures that consist of the combination of a berm and a crest wall.

3. Physical model tests

3.1. Test programme

The physical model tests were performed in the Scheldt Flume (110 m long, 1 m wide, and 1.2 m high) at Deltares. The wave generator is equipped with active reflection compensation. This means that the motion of the wave paddle compensates for the waves reflected by the structure preventing them to re-reflect at the wave paddle and propagate towards the model.

Four configurations of rubble mound breakwaters were tested:

1) Without a crest wall and without a berm
2) With a **crest wall** and without a berm
3) Without a crest wall and with a **berm**
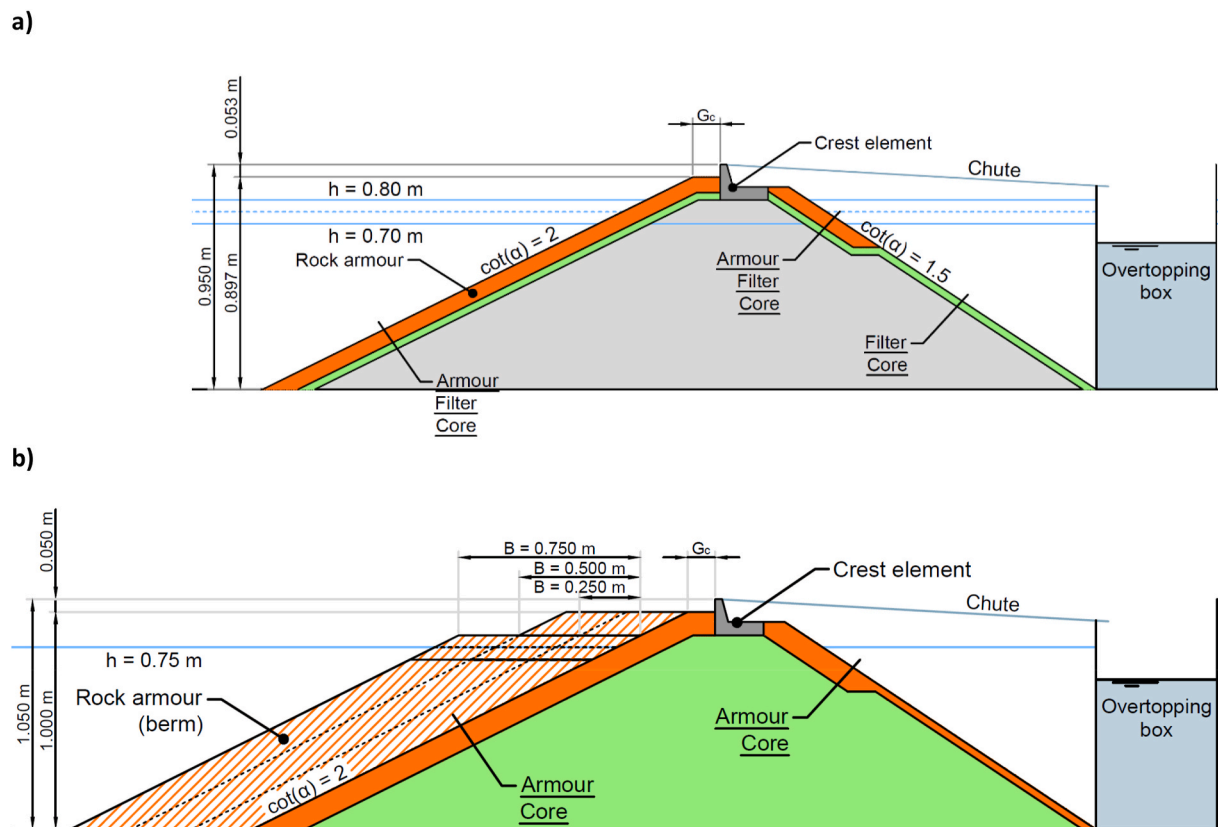4) With a **crest wall** and with a **berm**

Fig. 4. Cross-sections of tested structures; Panel a: example of structure with filter layer (Configuration 2), Panel b: example of structure without a filter layer (Configuration 4).

Fig. 4 shows examples of cross-sections that were tested (all with a horizontal foreshore). For the first two configurations two types of cross-sections were tested, one with a filter layer and one without a filter layer. All cross-sections had a 1:2 slope. The structure without a filter layer (for Configurations 1 to 4; Fig. 4b) consisted of a core ($D_{n50} = 16$ mm) and an armour layer ($D_{n50} = 38$ mm) with a thickness of $2D_{n50}$. The structure with a filter layer (for Configurations 1 and 2; Fig. 4a) consisted of a core ($D_{n50} = 6.4$ mm), a filter layer ($D_{n50} = 16$ mm), and an armour layer ($D_{n50} = 32$ mm) with a thickness of $2D_{n50}$. For Configuration 4 three berm widths were tested ($B = 0.25$ m, 0.50 m and 0.75 m; Fig. 4b) while for this structure without a filter layer also reference tests without a berm ($B = 0$ m) were performed (Configuration 2), to assess the effects of the berms irrespective of a potential influence of somewhat different core material. Thus, Configurations 1 and 2 were tested for the cross-sections with and without a filter layer, while Configurations 3 and 4 were tested only for the cross-section without a filter layer (see also Fig. 6). Seven different levels of the berm relative to the still water level (berm depths $h_b = -0.250$ m, -0.05 m, -0.025 m, 0 m, 0.025 m, 0.05 m and 0.075 m) were applied. The rubble mound berm (Fig. 4b) consisted of the armour material. Note that rubble mound structures are often placed in shallower water rather than in the deep-water conditions applied in the present tests, such that the amount of armour material in the berm would be significantly less than applied in the tests. Although the relatively large permeability of the berm has a stabilizing effect on the stability of the armour, it is unknown whether the permeability of berm consisting of armour material would affect the overtopping discharges compared to a berm that consists of a double layer of armour material and filter material underneath. The structures without a berm (Configurations 1 and 2) were tested with and without a filter (Fig. 4a and b), corresponding to structures with smaller and larger core material, but no clear effect on the wave overtopping discharges was observed. The L-shaped crest walls were positioned on top of the core material. No recurved parapet (bullnose) was applied on the crest wall.

The incident waves were measured by using five wave gauges from which the incident waves were derived using the method by Zelt and Skjelbreia (1992). The last wave gauge was positioned 8 m from the crest wall, while the crest wall was position at 41.8 m from the wave board; see Fig. 5 for a schematised overview of the structure in the wave flume. The mean overtopping discharges were measured by collecting the overtopping water via an overtopping chute into an overtopping box (for the configurations without the protruding crest wall the chute started at the same position as for those with a protruding crest wall).

The spectral significant wave height H_{m0} and the spectral wave period $T_{m-1,0}$ were obtained from the measured wave energy spectra at the toe. In all tests a JONSWAP wave spectrum (with a peak enhancement factor of 3.3) has been applied. All tests have been performed with 1000 waves. The wave steepness was varied. Incident wave heights were in the range between $H_{m0} = 0.078$ m and 0.224 m and the wave steepness at the toe of the structures were in the range between $s_{m-1,0} = 0.013$ and $s_{m-1,0} = 0.042$. Four water depths were applied (*i.e.* 0.70 m, 0.75 m, 0.775 m and 0.80 m), leading to various levels of the freeboard (R_c). The freeboard was in the range between $0.77 \leq R_c/H_{m0} \leq 1.76$. In total 171 tests resulted in wave overtopping. Table 1 shows the ranges of the most important parameters of the test programme.

3.2. Test results

In all panels of Fig. 7 the non-dimensional wave overtopping discharge is shown as function of the non-dimensional freeboard. For all four types of structures (1: no crest wall and no berm; 2: with crest wall, but no berm; 3: without crest wall, but with berm; 4: with crest wall and with berm), the upper two panels consistently show that the lower wave steepness leads to more wave overtopping than the higher wave steepness for the same non-dimensional freeboard (all filled symbols are above the open symbols of the same colour). In the upper right panel results are shown for configurations with a berm $B = 0.50$ m. For the configurations with a berm (upper right panel) the variations in wave overtopping due to a different wave steepness are larger than for the configurations without a berm (upper left panel).

The upper two panels of Fig. 7 also show that for the same non-dimensional freeboard the structures with a crest wall lead to more wave overtopping (the green lines are consistently above the red lines in the left panel, and the black lines are consistently above the blue lines in the right panel). Apparently, the roughness and permeability of the armour layers lead to more reduction than if the upper part of the structures are replaced by a smooth (impermeable) crest wall.

The two panels in the middle of Fig. 7 show the influence of the berm width (for structures with a crest wall); the left panel for the lower wave steepness and the right panel for the higher wave steepness. Both panels clearly show that a wider berm leads to less wave overtopping for the same non-dimensional freeboard. The reducing effect of the berm is larger for the higher wave steepness.

The lower two panels of Fig. 7 show the influence of the level of the berm; the left panel for a structure without a crest wall and the right panel for a structure with a crest wall. For the lower wave steepness there is a relatively small influence of the level of the berm; the higher berm (emerged) leads to slightly less wave overtopping than the berm at the still water level (mid) and the lowest berm (submerged). For the higher wave steepness there is a larger influence of the berm level, again with an emerged berm leading to the lowest overtopping discharges.

The results shown in Fig. 7 indicate that the influence of the wave steepness, the influence of the crest wall, and the influence of the berm cannot be ignored for assessing wave overtopping discharges.

4. Analysis of test results

4.1. Introduction to analysis

As described in Section 3.2, the test results clearly show that the wave steepness, a berm, and a crest wall, all affect the wave overtopping discharge. Consequently, expressions proposed in existing design guidelines such as TAW (2002) or EurOtop (2018) cannot be used to accurately describe wave overtopping at rubble mound breakwaters.

Lioutas et al. (2012) and Koosheh et al. (2022) showed that wave overtopping at rock armoured slopes with an impermeable core is affected by the wave steepness. The present tests show (see Fig. 7) that this is also valid for rock armoured structures with a permeable core. In Eq. (2) by Koosheh et al. (2022) for rock armoured slopes with an impermeable core, the wave steepness is incorporated using the wave steepness in the exponential part of the expression to the power $d = 0.35$. For the present tests the optimal power of the wave steepness
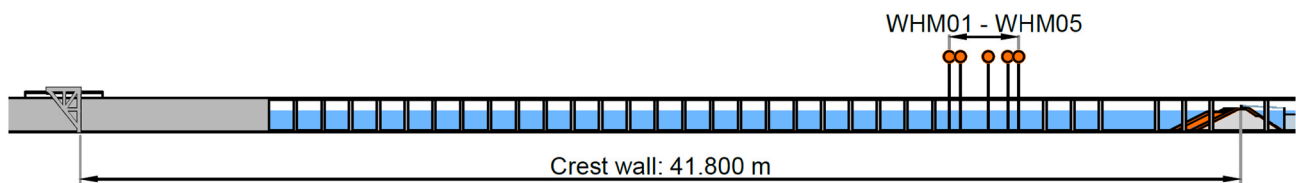
WHM01 - WHM05

Crest wall: 41.800 m

Fig. 5. Overview of tested structure in wave flume.

Fig. 6. Pictures of waves on a rubble mound breakwater with a berm and a crest wall (Configuration 4; $B = 0.75$ m, $R_c = 0.3$ m, $H_{m0} = 0.224$ m, $s_{m-1,0} = 0.023$).

in the exponential part would be lower (about $d = 0.15$) for fully permeable rubble mound breakwaters. Since here the intention is to obtain a set of expressions that is valid for rubble mound breakwaters (with a permeable core) with or without a berm and/or a crest wall, a more accurate expression has been developed to account for effects of the wave steepness, a berm, a crest wall, and a combination of a crest wall and a berm.

4.2. Wave overtopping expression

The following expression is proposed to described wave overtopping at rubble mound breakwaters:

$$\frac{q}{\sqrt{gH_{m0}^3}} = 0.016 \ s_{m-1,0}^{-1} \ \exp\left[-\frac{2.4 \ R_c}{\gamma_f \ \gamma_b \ \gamma_\beta \ \gamma_v \ \gamma_p \ H_{m0}} \right] \tag{3}$$

The following sections deal with the influence factors for roughness

(γ_f), a berm (γ_b), a crest wall (γ_v), and oblique waves (γ_β). To account for the influence of a recurved parapet (γ_p) at a crest wall of rubble mound breakwaters, reference is made to Oh et al. (2018). Obviously, if no recurved parapet is present then $\gamma_p = 1$.

To account for the influence of wind at rubble mound breakwaters with a crest wall, reference is made to Wolters and Van Gent (2007). The influence of wind increases the discharge as calculated using Eq. (3) by a maximum value between 1.2 and 4.7. Although wind can increase the wave overtopping discharge, in practice the influence of wind is usually not accounted for.

If besides the wave conditions that cause wave overtopping also swell from another direction is present, the effect of swell can be accounted for by reducing the freeboard R_c in Eq. (3) with a value c_{swell} = 0.4 to 0.5 times the significant wave height of the swell component (R_c - $c_{swell} H_{m0-swell}$), irrespective of the direction of the swell component. For dikes and caisson breakwaters guidance on such crossing sea states is provided by Van der Werf and Van Gent (2018) for dikes ($c_{swell} = 0.5$)

Table 1
Parameter ranges of the test programme.

Parameter	Symbol	Values/Ranges
Seaward slope (−)	$\cot \alpha$	2
Armour stone diameter (m)	D_{n50}	0.032 & 0.038
Water depth (m)	h	0.700–0.800
Incident significant wave height at toe (m)	H_{m0}	0.074–0.224
Wave steepness: $s_{m-1,0}=2\pi H_{m0}/gT_{m-1,0}^2$ (−)	$s_{m-1,0}$	0.013–0.042
Surf-similarity parameter: $\xi_{m-1,0}=\tan \alpha/s_{m-1,0}^{0.5}$ (−)	$\xi_{m-1,0}$	2.45–4.38
Number of waves (−)	N	1000
Freeboard (m)	R_c	0.10–0.30
Level of armour in front of crest wall (m)	A_c	0.10–0.25
Width of armour in front of crest wall (m)	G_c	0.11–0.15
Berm width (m)	B	0–0.75
Berm depth (negative is a berm above SWL) (m)	h_b	−0.25–0.075
Non-dimensional freeboard	R_c/H_{m0}	0.77–2.10
Non-dimensional level of armour at crest	A_c/H_{m0}	0.77–1.76
Non-dimensional protruding part of crest wall	$(R_c\text{-}A_c)/H_{m0}$	0.00–0.68
Ratio of protruding part of crest wall and freeboard (−)	$(R_c\text{-}A_c)/R_c$	0.00–0.35
Non-dimensional width of armour in front of crest wall	G_c/H_{m0}	0.67–1.46
Non-dimensional berm width	B/H_{m0}	0.00–5.24
Non-dimensional berm depth	h_b/H_{m0}	−1.73–0.52
Non-dimensional berm level relative to armour crest: $B_L=A_c+h_b$	B_L/H_{m0}	0.00–2.09
Non-dimensional stone diameter	D_{n50}/H_{m0}	0.17–0.41

and by Van Gent (2021) for caisson breakwaters ($c_{swell} = 0.4$). Although not tested for rubble mound breakwaters, a value between those for gentle sloping dikes and vertical caisson breakwaters is considered a reasonable estimate ($c_{swell} = 0.45$).

The coefficients in Eq. (3) have been calibrated based on the present tests. The accuracy of the expression using these coefficients will be discussed in a following section. Note that the wave steepness as incorporated in Eq. (3) causes that a condition with a twice larger wave length ($L_{m-1,0}$) leads to twice more overtopping, for surging waves with equal wave heights. If the overtopping discharge q is made non-dimensional by using $L_{m-1,0}\sqrt{(gH_{m0})}$ instead of $\sqrt{(gH_{m0}^3)}$, the wave steepness disappears from Eq. (3) while the rest of the expression and coefficients remains the same.

4.3. Influence factors

To account for the influence of roughness (γ_f), the influence of a crest wall (γ_v), the influence of a berm (γ_b), and the influence of oblique waves (γ_β), the following expressions are developed and discussed:

$$\gamma_f = 1 - 0.7 \left(\frac{D_{n50}}{H_{m0}}\right)^{0.1} \tag{4}$$

$$\gamma_v = 1 + 0.45 \left(\frac{R_c - A_c}{R_c}\right) \tag{5}$$

$$\gamma_b = 1 - 18 \left(\frac{s_{m-1,0} B}{H_{m0}}\right)^{1.3} \left(1 - 0.34 \left(\frac{B_L}{s_{m-1,0} A_c}\right)^{0.2}\right) \tag{6}$$

$$\gamma_\beta = 0.65 \cos^2\beta + 0.35 \tag{7}$$

where D_{n50} is the diameter of the stones in the armour layer, R_c - A_c is the protruding part of the crest wall (see also Fig. 3), B is the width of the berm, B_L is the vertical distance between the level of the berm and the level of the armour layer at the crest ($B_L = A_c + h_b$), and β is the angle of wave incidence ($\beta = 0°$ for perpendicular wave attack). In the following, these expressions for influence factors are discussed and presented together with data. The expression for the influence factor for oblique waves (Eq. (7)) was proposed by Van Gent and Van der Werf (2019) for rubble mound breakwaters with a crest wall and their data is applied in combination with the newly derived set of expressions (Eqs. (3)–(7)). The influence factor for a recurved parapet (γ_p) is 1.

4.3.1. Roughness

For wave overtopping at rock armour layers with a layer thickness of about two diameters constant roughness factors have been proposed in literature in the range between $\gamma_f = 0.4$ to 0.5 (see also Bruce et al., 2009; Molines and Medina, 2015, and Eldrup and Lykke Andersen, 2018). For impermeable slopes dependencies of the roughness on the amount of overtopping, on the freeboard, the wave steepness, the surf-similarity parameter, and height of protruding blocks have been found (see for instance Capel, 2015, and Chen et al., 2020). Here, a relatively simple expression that only depends on the non-dimensional stone diameter (D_{n50}/H_{m0}) is proposed, where in the present tests this ratio varied between 0.17 and 0.41, leading to $\gamma_f = 0.36$ to 0.41 using Eq. (4); the lower values of this range of the influence factor γ_f correspond to the tests with lowest waves in the test programme, while the higher values correspond to higher waves and lead to a ratio that matches with existing design guidelines with (constant) roughness factors for rock armour layers of two diameters thick.

Fig. 8 shows the measured overtopping discharges versus the calculated discharges using Eqs. (3) and (4), for the structures without a berm and without a crest wall. Fig. 8 shows that Eqs. (3) and (4) describe the data reasonably well, thus with the influence of the wave steepness incorporated as shown in Eq. (3).

For the comparison of the measurements with the described prediction formulae use is made of the following error-measure, referred to as RMSE:

$$\text{RMSE} = \sqrt{\frac{\sum_{i=1}^{n_{tests}} \left(\log(Q_{measured}) - \log(Q_{calculated})\right)^2}{n_{tests}}} \tag{8}$$

where n_{tests} is the number of tests on which the RMSE is based, Q are the non-dimensional values of the measured and calculated overtopping discharges [$Q = q/(gH_{m0}^3)^{0.5}$]. The RMSE is only based on measured overtopping values larger than $Q_{measured} \geq 10^{-6}$ since smaller values are often less relevant and scale effects may be present.

Table 2 show the RMSE values for both structure types (with and without a filter) without a crest wall and without a berm. Table 2 shows that incorporating the non-dimensional stone diameter as expressed by Eq. (3) improves the predictions compared to the use of a constant value for the influence of the roughness ($\gamma_f = 0.4$), where the applied value is the optimal value if a constant value is used in combination with the earlier mentioned coefficients used in Eq. (3).
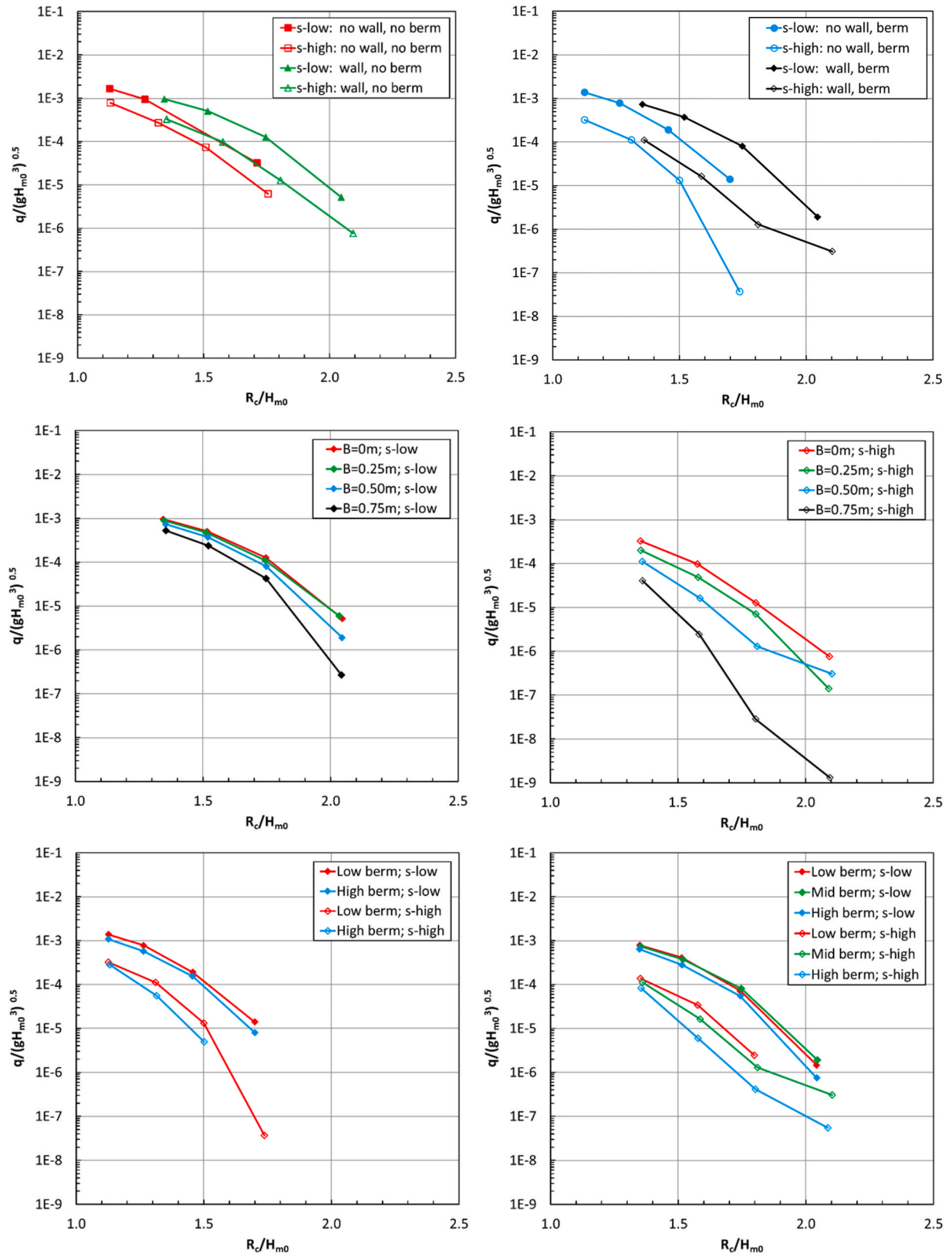
Fig. 7. Influence of wave steepness (upper panels), influence of berm width (mid panels; with crest wall), and influence of the berm level (lower panels; without and with crest wall respectively).
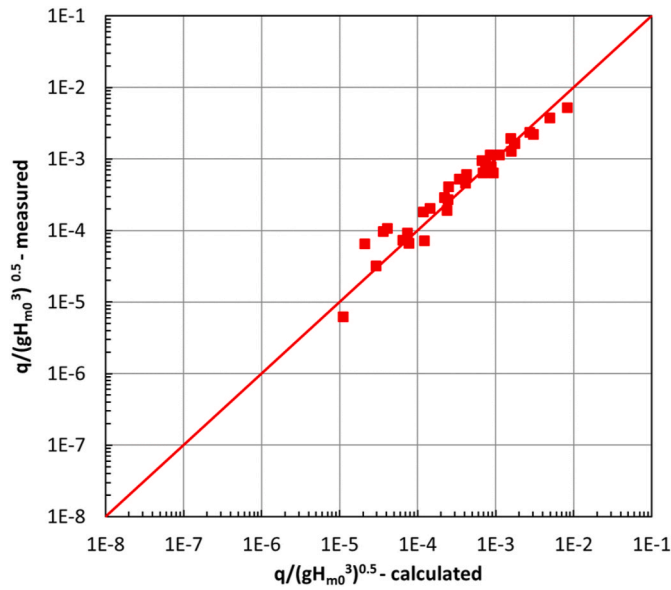
Fig. 8. Measured versus calculated wave overtopping discharge using Eqs. (3) and (4).

Table 2
RMSE for structures without a crest wall and without a berm.

Prediction method	RMSE		
	No filter	With filter	Mean
No crest wall, no berm: Eq. (3) with $\gamma_f = 0.4$	0.1826	0.2248	0.2037
No crest wall, no berm: Eq. (3) and Eq. 4	0.1172	0.1921	0.1547

4.3.2. Crest wall

For the same crest level (same R_c) a rubble mound structure with a crest wall leads to more wave overtopping than for a rubble mound structure where the armour layer is extended to the top of the structure ($A_c = R_c$), at least for the structures tested in the present test programme where the armour layer has a horizontal part in front of the crest wall ($0.67 \leq G_c/H_{m0} \leq 1.46$), while the crest wall did not have a recurved
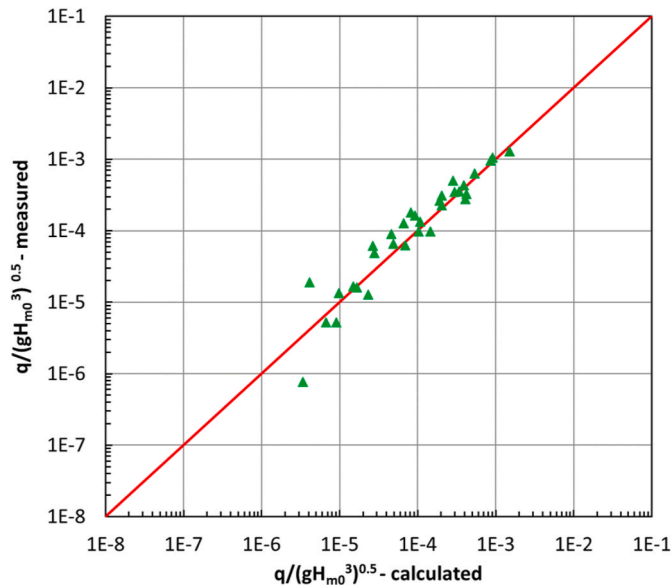

Fig. 9. Measured versus calculated wave overtopping discharge using Eqs. (3)–(5).

Table 3
RMSE for structures with a crest wall but without a berm.

Prediction method	RMSE		
	No filter	With filter	Mean
Crest wall, no berm: Eqs. (3)–(5)	0.2009	0.2137	0.2073

parapet ($\gamma_p = 1$). The reduction due to the roughness and permeability of the upper part of the slope is larger than the reduction due to the crest wall (without a recurved parapet). During the tests it was observed that once the wave run-up front reaches the crest wall, there is a clear effect of the crest wall with a clear vertical velocity component of the water hitting the crest wall. However, once the space in front of the crest wall is filled with water, the rest of the wave reaching the crest relatively easily overtops the structure. The upper panels of Fig. 7 show that the structures with a crest wall lead to more overtopping than the corresponding structures with the same crest elevation. Therefore, for rubble mound structures, the influence factor for crest walls γ_v becomes a value larger than one. Eq. (5) shows a simple relation where the influence of the crest wall is incorporated by using a linear relation with the ratio of the protruding part of the crest wall ($R_c - A_c$) and the crest elevation (R_c).

Fig. 9 shows the measured overtopping discharges versus the calculated discharges using Eqs. (3)–(5), for the structures with a crest wall but without a berm. Fig. 9 shows that Eqs. (3)–(5) describe the data reasonably well. Table 3 show the RMSE values for both structure types (with and without a filter) with a crest wall but without a berm (for $Q_{measured} \geq 10^{-6}$).

4.3.3. Berm

As shown in Fig. 7 (two panels in the middle) the larger the berm width B, the larger the reduction in overtopping discharge. This effect is stronger for the conditions with a high wave steepness, which means that the same berm width reduces the overtopping more for conditions with a shorter wave length. Since the wave steepness (or wave length) affects the importance of the width of the berm, the wave steepness is incorporated in the expression to account for the width of the berm. Note that the effect of the berm width as expressed by Eq. (6) using "$s_{m-1,0}B/H_{m0}$" can be rewritten to "$B/L_{m-1,0}$", thus the ratio between the berm width and the wave length determines the effects of the berm width.

Fig. 7 also shows that the level of the berm has an influence, where the berm at the highest level reduces the overtopping discharge more than the berms at a lower level. The test programme also includes tests with the level of the "berm" at the level of the crest of the armour layer in front of the crest wall ($h_b = -A_c$ and $B = 0.25$ m and $B = 0.5$ m). These tests confirm that the higher the level of the berm, the lower the wave overtopping discharge. This is in contrast to the influence of impermeable berms at dikes, where the berm at the level of the still water level has the maximum reducing effect (see for instance Chen et al., 2020, 2021). A permeable berm has another effect than an impermeable berm, because a permeable berm at a higher level (thus with a larger amount of stones) causes more reduction due to more infiltration of up rushing water into the berm and more dissipation of wave energy inside the permeable berm. The level of the berm is incorporated by using an expression based on the vertical distance between the horizontal part of the armour layer at the top (A_c *w.r.t.* the SWL) and the level of the berm (h_b *w.r.t.* SWL) such that the reduction due to the level of the berm is proportional to $B_L = A_c + h_b$, thus with the largest influence of a berm for a berm at the highest level. Since the wave steepness affects the importance of the level of the berm, the wave steepness is incorporated in the expression to account for the level of the berm.

Thus, the width of the berm, level of the berm, and the wave steepness affect the reducing effect of a berm on wave overtopping discharges. This is expressed in Eq. (6), where the coefficients have been calibrated based on the present tests.
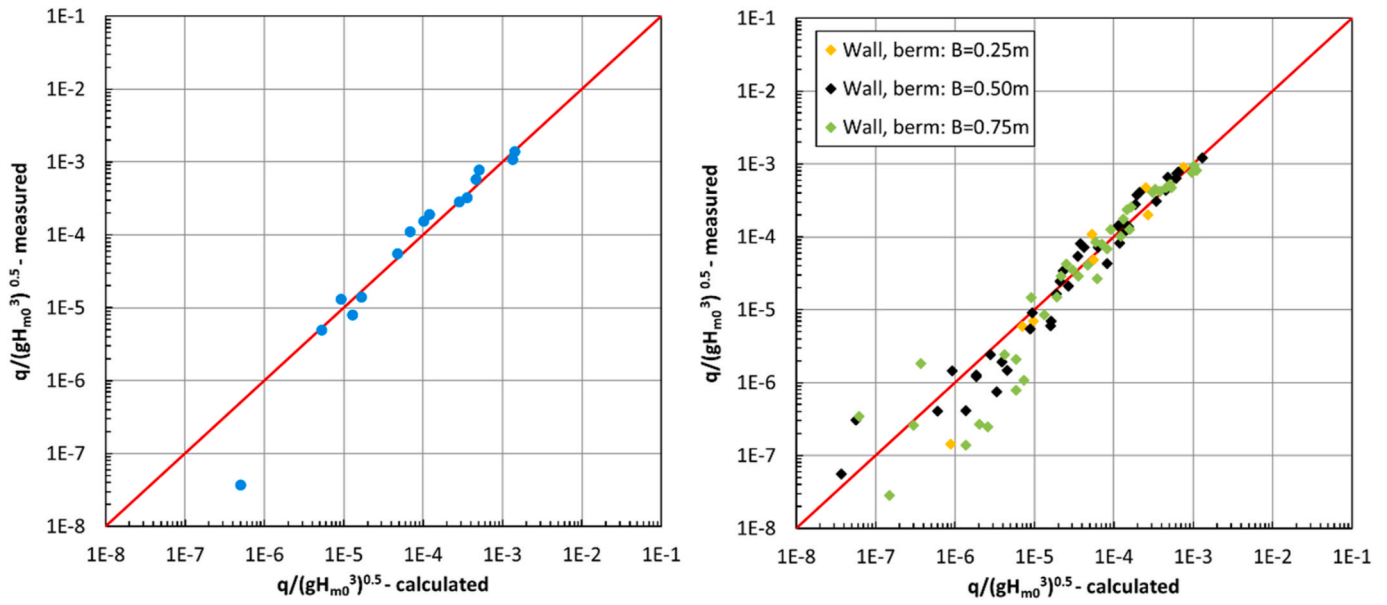
Fig. 10. Measured versus calculated wave overtopping discharge using Eqs. (3)–(6); left panel shows the data for the structures with a berm but without a crest wall; right panel shows the data for the structures with a berm and with a crest wall.

Table 4
RMSE for structures with a berm (without and with a crest wall).

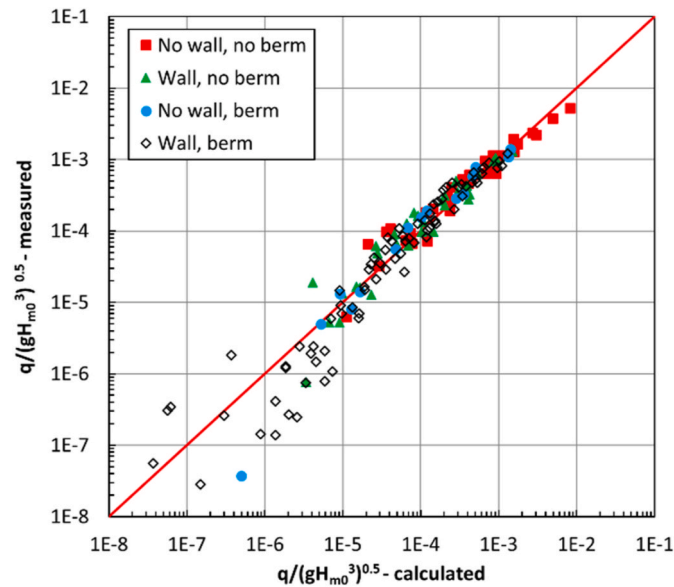| Prediction method	RMSE		
	Without wall	With wall	Mean
Berm: Eqs. (3)–(6)	0.1331	0.2219	0.1775

Fig. 11. Measured versus calculated wave overtopping discharge using Eqs. (3)–(6).

Fig. 10 shows the measured overtopping discharges versus the calculated discharges using Eqs. (3)–(6), for the structures with a berm, without and with a crest wall. The left panel shows the tests for a structure without a filter layer and the right panel the tests for the structure without a filter layer. Both graphs show that Eqs. (3)–(6) describe the data reasonably well. Table 4 show the RMSE values for all structures with a berm, either without or with crest wall (for

$Q_{measured} \geq 10^{-6}$). Fig. 10 illustrates that the largest deviations between measured and calculated discharges are for low discharges measured at the structure with the widest berm and a crest wall. Nevertheless, the match between the measured and calculated discharges is rather good, as illustrated by the RMSE shown in Table 4. Fig. 11 shows all data from the presented test programme for all structure types.

4.3.4. Oblique waves

The presented tests so far are all for perpendicular wave attack. In Van Gent and Van der Werf (2019) a rubble mound breakwater with a crest wall, with a cross-section shown in the upper panel of Fig. 4, was tested to study the influence of oblique waves. Based on those tests, the influence of oblique waves was described by Eq. (7). As an independent check of the validity of Eqs. (3)–(5) in combination with Eq. (7) to account for oblique waves, those data are used here. Note that for those tests also the non-dimensional stone diameter (D_{n50}/H_{m0}) was varied over a wider range (0.20–0.62, leading to $\gamma_f = 0.33$ to 0.40), than for the presented test programme.

The left panel of Fig. 12 shows the data by Van Gent and Van der Werf (2019) while the right panel shows these data in combination with the data from the presented test programme. Fig. 12 shows that the largest deviation between measured and calculated discharges are for the conditions with the most oblique waves. However, for the discharges that are in a relevant range (for $Q_{measured} \geq 10^{-6}$), the agreement is rather good. The corresponding RMSE value is 0.6157, which is clearly larger than those obtained for the previously discussed influence factors based on perpendicular wave attack.

4.4. Discussion

Based on the data described in previous sections the set of expressions (Eqs. (3)–(7)) has been derived. Table 1 shows the ranges of the most important parameters. Although these ranges cover a rather wide range of rubble mound structures, there are relevant limitations with respect to the ranges of validity. Although the expressions may be accurate outside the range of the test conditions, the validity is unknown. Some important limitations and other aspects are discussed below.

- **Shallow foreshores**: The derived expressions (Eqs. (3)–(7)) are all based on conditions where no significant wave breaking occurs on
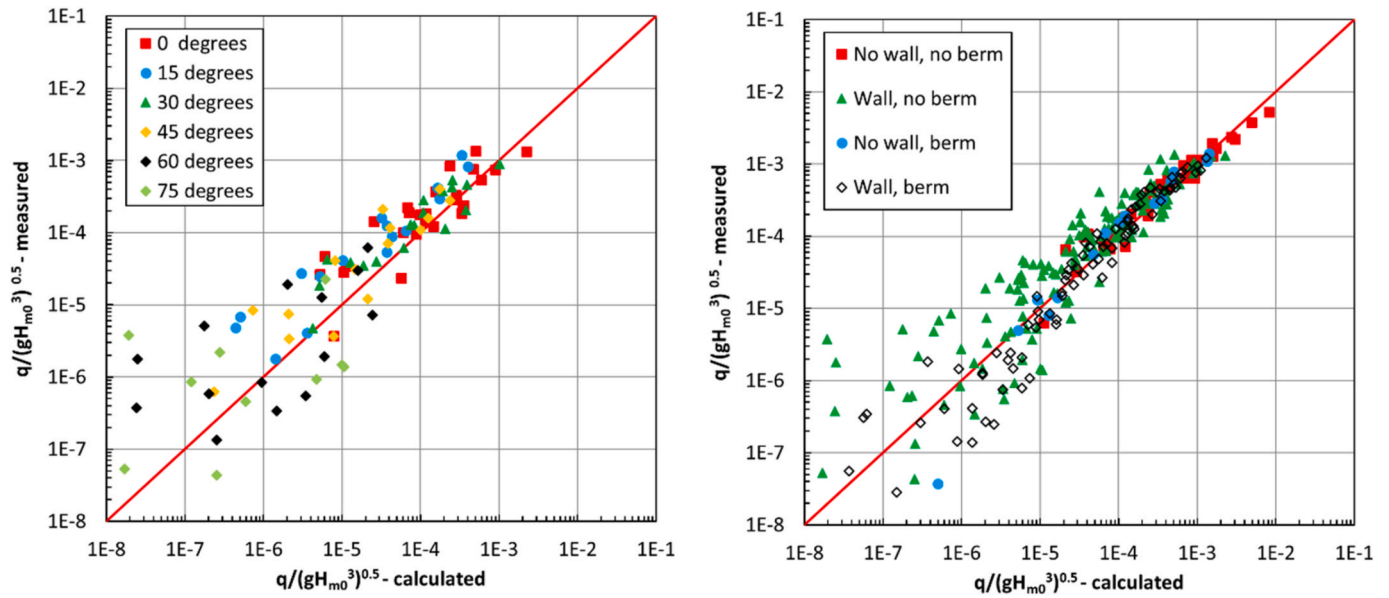
Fig. 12. Measured versus calculated wave overtopping discharge using Eqs. (3)–(7); left panel shows the data by Van Gent and Van der Werf (2019) obtained to study oblique waves; right panel shows these data (green triangles) plus all data from the presented test programme.

the foreshore. Since rubble mound structure are often in relative shallow water, this limitation can be important. For instance, the expression describing the influence of oblique waves (Eq. (7)) leads to a significant reduction in wave overtopping discharge for very oblique waves. It is not unlikely that for conditions where significant wave breaking occurs before the waves reach the structure, the reductive influence may be less than obtained for the deeper water conditions on which the expression is based (Eq. (7)). In addition, also wave refraction plays a larger role in shallow water. It is recommended to study the influence of oblique waves on wave overtopping discharges if such conditions with wave breaking on the foreshore are present.

- **Berm**: The derived set of expressions is based on a data set that does not contain a combination of oblique waves and rubble mound structures with a berm. In Van Gent (2020) and Chen et al. (2022) the influence of oblique waves on wave overtopping was studied for impermeable structures with a berm. It was shown that the reductive influence of the berm is larger for oblique waves, more than the combination of the two separate influence factors for oblique waves and for a berm would suggest. It is not unlikely that also for rubble mound breakwaters the influence of a berm is larger for oblique waves, larger than the present set of expressions would predict. Nevertheless, the present set of expressions provides conservative estimates for rubble mound structures with a berm under oblique wave attack in conditions without severe wave breaking on the foreshore.

  For partly or hardly reshaping berm breakwaters an expression to account for the effect of a berm was proposed by Sigurdarson and van der Meer (2012). They proposed to replace the influence factor for roughness by a factor that accounts for the berm. This expression contains the wave steepness and the berm width but not the influence of the level of a berm. Applying this expression for partly and hardly reshaping berm breakwaters for the tested statically stable rubble mound breakwaters with a berm shows that the expression for partly and hardly reshaping berm breakwaters clearly underestimates the reductive effects of a berm on wave overtopping discharges for the tested breakwaters with a berm.

- **Slope angle**: The derived expressions are obtained based on tests with a 1:2 slope. This is a very common slope for rubble mound
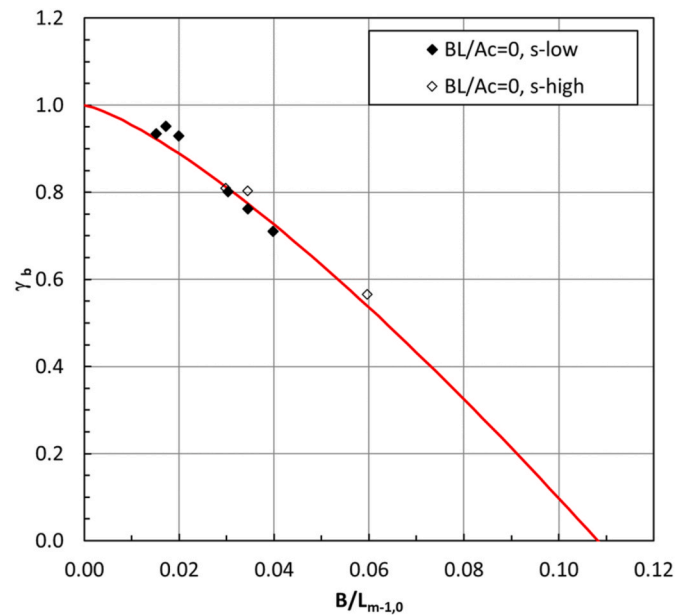

Fig. 13. Expression and data for the influence of the width of the armour in front of the crest wall ($B_L = 0$ in Eq. (6)) and the data on "berms" of $B = 0.25$ m and $B = 0.5$ m at the level of the armour in front of the crest).

structures. To what extend the expressions are valid for other slopes such a 1:1.5 or 1:3 needs to be validated.

- **Width of armour in front of crest wall** (G_c): For the width of the armour in front of a crest wall, a rather common width has been applied in the described test programme (G_c is about four stone diameters wide). However, for structures where this width is larger, the reduction in discharge is larger (see also Besley, 1999). In the present test programme also tests with a "berm" at the level of the armour at the crest have been performed (up to $G_c + B = 0.65$ m). For these tests Eq. (6) matches rather well with the data for wide crests, see Fig. 13 (for $Q_{measured} \geq 10^{-6}$). Eq. (6) can therefore be used to estimate the effect of larger width of the armour in front of a crest wall (thus using $B_L = 0$ in Eq. (6)).

- **Recurved parapet**: The derived expressions are obtained for a crest wall without a recurved parapet. A recurved parapet can reduce the wave overtopping discharge considerably, especially for relatively low overtopping discharges (see for instance Oh et al., 2018). However, it is likely that the effect of a recurved parapet reduces for very oblique waves (see Van Gent, 2021).

- **Armour layer**: The derived expressions are obtained for rock armoured structures with a permeable core. For a structure with an impermeable core reference is made to Koosheh et al. (2022). However, their method does not provide expressions for rock armoured structures with a crest wall or a berm for structures with an impermeable core. Structures with concrete armour layers have not been tested in the presented test programme. If the roughness of the concrete elements is incorporated in the influence factor for the roughness, this is assumed not to lead to significantly different results than those for rock armoured slopes. Information on roughness factors for various armour layers is provided by Bruce et al. (2009).

- **Overtopping parameters**: The presented set of influence factors for roughness, crest walls, berms and oblique waves have been derived only for wave overtopping discharges. These influence factors are not necessarily valid for other overtopping parameter such as the overtopping volume per overtopping wave, percentages of overtopping waves, and flow velocities and the flow depth during overtopping events. For information on overtopping volumes reference is made to Mares-Nasarre et al. (2020) for conditions with breaking waves, and Koosheh et al. (2021). For information on reductive effects on flow velocities and the flow depth during overtopping events, reference is made to Chen et al. (2022).

- **Data-driven methods:** Using the derived expressions leads to a RMSE of 0.2038 for all described data from the wave flume experiments for $Q_{measured} \geq 10^{-6}$. If the existing machine-learning methods by Van Gent et al. (2007) or Den Bieman et al. (2021) are used to estimate the discharges for the tested conditions, the RMSE are 0.6359 and 0.5846 respectively. These values are higher than for the expressions derived from the described tests. This is probably partly caused by the data sets on which these methods are based; in the applied data sets limited data is present for rubble mound breakwaters that both contain a berm and a protruding crest wall. An update of machine-learning methods by using the presented data can further improve the quality of the predictions by machine learning methods.

The ranges of the parameters in the test programme also lead to limitations of some of the derived influence factors. Outside these ranges the accuracy of the expressions is unknown. For the influence factor for the roughness, values larger than $\gamma_f > 0.33$ have been obtained; it is recommend not to apply values lower than $\gamma_f = 0.33$ for rock armoured slopes without additional validation. The ratio of the protruding part of the crest wall and the freeboard $(R_c - A_c)/R_c$ was smaller than 0.35 in the present test programme. This leads to a maximum influence factor for the crest wall of $\gamma_v = 1.16$. Although tested for a wide range of berm widths, berm levels and wave steepness, the influence factor for the berm was not lower than 0.5 in the present test programme (those tests that would result in lower values led to zero wave overtopping). It is recommended not to apply an influence factor for the berm outside the range $0.5 \leq \gamma_b \leq 1$ without additional validation.

5. Conclusions and recommendations

The described physical model tests to study wave overtopping discharges at rubble mound breakwaters have led to the following conclusions:

- Wave overtopping discharges at rubble mound breakwaters depend on the wave steepness.

- For rubble mound breakwaters with the same crest elevation, the wave overtopping discharges are larger for breakwaters with a crest wall than those without a crest wall. Obviously, adding a protruding crest wall to a rubble mound breakwater, thus increasing the crest elevation, leads to a reduction in discharges.

- The effect of a crest wall at rubble mound breakwaters can be incorporated in the prediction of wave overtopping discharges by using the relative height of the protruding part of a crest wall. The proposed influence factor accurately describes the effects of the crest walls used in the performed tests.

- A stable berm at the seaward slope of a rubble mound breakwater reduces wave overtopping. The effect of a stable berm is affected by the berm width, the level of the berm, and the wave steepness. The proposed influence factor for a berm accurately describes the effects of the berms used in the performed tests.

- For structures with both a crest wall and with a berm, the combined influence can be accounted for by multiplying the individual effects of the crest wall and the berm.

- The developed set of expressions for wave overtopping at rubble mound structures has also been validated based on existing data for oblique wave attack on rubble mound breakwaters with a crest wall. The match between the data on oblique wave attack and the derived expressions is reasonable.

- Incorporating or modifying a crest wall or a berm can be effective to reduce wave overtopping. This is not only important for the design of rubble mound breakwaters but also for climate adaptation of existing rubble mound breakwaters to account for the effects of sea level rise. The set of expressions derived based on the present physical model tests can contribute to the design of rubble mound breakwaters and to the assessment of the optimal adaptation of existing breakwaters.

The physical model tests used to develop and validate the derived set of expressions are performed over a fairly wide range of relevant parameters. However, the validity of the derived expressions for applications where waves break before reaching the structure, is yet unknown. This limits the applicability for rubble mound breakwaters in shallow water. It is recommended to perform such validation for applications with shallow foreshores, as well as to study the effects of berms on wave overtopping at rubble mound breakwaters for oblique wave attack. It is also recommended to further investigate the influence of recurved parapets on crest walls of rubble mound breakwaters and the influence of armour layers that consist of concrete armour units rather than rock. Furthermore, it is recommended to study the influence of crest walls and berms on volumes per overtopping wave, on percentages of overtopping waves, and on flow velocities and the flow depth during overtopping events.

CRediT authorship contribution statement

Marcel R.A. van Gent: Conceptualization, Methodology, Investigation, Formal analysis, Data curation, Visualization, Writing – original draft. **Guido Wolters:** Investigation, Writing – review & editing. **Alex Capel:** Investigation, Writing – review & editing.

Declaration of competing interest

The authors declare that they have no known competing financial interests or personal relationships that could have appeared to influence the work reported in this paper.

Acknowledgements

References

Battjes, J.A., 1974. Computation of Set-Up, Longshore Currents, Run-Up and Overtopping Due to Wind-Generated Waves. Ph.D.-thesis. TU Delft.

Besley, P., 1999. Overtopping of Seawalls, Design and Assessment Manual, HR Wallingford R&D Technical Report W178.

Bruce, T., Van der Meer, J.W., Franco, L., Pearson, J.M., 2009. Overtopping performance of different armour units for rubble mound breakwaters. Coast Eng. 56, 166–179.

Capel, A., 2015. Wave run-up and overtopping reduction by block revetments with enhanced roughness. Coast Eng. 104, 76–92. https://doi.org/10.1016/j.coastaleng.2015.06.007.

Chen, W., Van Gent, M.R.A., Warmink, J.J., Hulscher, S.J.M.H., 2020. The influence of a berm and roughness on the wave overtopping at dikes. Coast Eng. 156 https://doi.org/10.1016/j.coastaleng.2019.103613.

Chen, W., Warmink, J.J., Van Gent, M.R.A., Hulscher, S.J.M.H., 2022. Numerical investigation of the effects of roughness, a berm and oblique waves on wave overtopping processes at dikes. Appl. Ocean Res. 118 https://doi.org/10.1016/j.apor.2021.102971.

Christensen, N.F., Røge, M.S., Thomsen, J.B., Andersen, T.L., Burcharth, H.F., Nørgaard, J.Q.H., 2014. Overtopping on rubble mound breakwaters for low steepness waves in deep and depth limited conditions. In: Proc. ICCE 2014, vol. 6. https://doi.org/10.9753/icce.v34.structures.6.

Den Bieman, J.P., Van Gent, M.R.A., Van den Boogaard, H.F.P., 2021. Wave overtopping predictions using an advanced machine learning technique. Coast Eng. https://doi.org/10.1016/j.coastaleng.2020.103830.

De Waal, J.P., van der Meer, J.W., 1992. Wave run-up and overtopping on coastal structures, ASCE. In: Proc. ICCE 1992, vol. 2, pp. 1758–1771.

Eldrup, M.R., Lykke Andersen, T., 2018. Recalibration of overtopping roughness factors of different armour types, Thomas Telford. In: Proc. Coasts, Marine Structures and Breakwaters 2017, Liverpool, pp. 1011–1020. https://doi.org/10.1680/cmsb.63174.1011.

EurOtop, 2018. In: van der Meer, J.W., Allsop, N.W.H., Bruce, T., de Rouck, J., Kortenhaus, A., Pullen, T., Schüttrumpf, H., Troch, P., Zanuttigh, B. (Eds.), Manual on Wave Overtopping of Sea Defences and Related Structures (incl. Errata November 2019). www.overtopping-manual.com.

Gallach Sánchez, D., 2018. Experimental Study of Wave Overtopping Performance of Steep Low-Crested Structures. Ph.D. Thesis. Universiteit Gent, Belgium.

Gallach-Sánchez, D., Troch, P., Kortenhaus, A., 2021. A new average wave overtopping prediction formula with improved accuracy for smooth steep low crested structures. Coast Eng. 163 https://doi.org/10.1016/j.coastaleng.2020.103800.

Goda, Y., 1971. Expected rate of irregular wave overtopping of seawalls. Coast Eng. Jpn. 14, 45–51 (JSCE, Tokyo).

Hogeveen, K.P.J., 2021. Climate Adaption of Rubble Mound Breakwaters; A Study to the Accuracy of Overtopping Formulas for Combination of Solutions. M.Sc. thesis. TU Delft, Delft. http://resolver.tudelft.nl/uuid:3a6ec8ac-0b81-4d32-adf1-6d7b4f842ceb.

Koosheh, A., Etemad-Shahidi, A., Cartwright, N., Tomlinson, R., Van Gent, M.R.A., 2021. Individual wave overtopping at coastal structures: A critical review and the existing challenges. Appl. Ocean Res. 106 https://doi.org/10.1016/j.apor.2020.102476. Elsevier.

Koosheh, A., Etemad-Shahidi, A., Cartwright, N., Tomlinson, R., Van Gent, M.R.A., 2022. Experimental study of wave overtopping at rubble mound seawalls. Coast. Eng. 172 https://doi.org/10.1016/j.coastaleng.2021.104062. Elsevier.

Krom, J., 2012. Wave Overtopping at Rubble Mound Breakwaters with a Non-reshaping Berm. M.Sc. thesis. TU Delft, Delft.

Lioutas, A.C., Smith, G.M., Verhagen, H.J., 2012. Spatial distribution of overtopping. Proc. ICCE. https://doi.org/10.9753/icce.v33.structures.63.

Mares-Nasarre, P., Molines, J., Gómez-Martin, M.E., Medina, J.R., 2020. Individual wave overtopping volumes on mound breakwaters in breaking wave conditions and gentle sea bottoms. Coast Eng. 159 https://doi.org/10.1016/j.coastaleng.2020.103703.

Mares-Nasarre, P., Molines, J., Gómez-Martin, M.E., Medina, J.R., 2021. Explicit Neural Network-derived formula for overtopping flow on mound breakwaters in depth-limited breaking wave conditions. Coast Eng. 164 https://doi.org/10.1016/j.coastaleng.2020.103810.

Molines, J., Medina, J.R., 2015. Calibration of overtopping roughness factors for concrete armour units in non-breaking conditions using the CLASH database. Coast Eng. 96, 62–70.

Molines, J., Medina, J.R., 2016. Explicit wave-overtopping formula for mound breakwaters with crown walls using CLASH Neural Network-derived data. J. Waterw. Port, Coast. Ocean Eng. 142 https://doi.org/10.1061/(ASCE)WW.1943-5460.0000322.

Oh, S.H., Jang, S.C., Lee, J., 2018. Wave overtopping and loading for the recurved parapets on the crest of rubble mound breakwater, ICE Conference Coasts. Mar. Struct. Breakwaters Liverp. https://doi.org/10.1680/cmsb.63174.0979.

Owen, M.W., 1980. Design of Seawalls Allowing for Wave Overtopping (Report No. Ex 924). Hydraul. Res. HR Wallingford.

Pillai, K., Etemad-Shahidi, A., Lemckert, C., 2017a. Wave overtopping at berm breakwaters: review and sensitivity analysis of prediction models. Coast Eng. 120, 1–21. https://doi.org/10.1016/j.coastaleng.2016.11.003.

Pillai, K., Etemad-Shahidi, A., Lemckert, C., 2017b. Wave overtopping at berm breakwaters: experimental study and development of prediction formula. Coast Eng. 130, 85–102. https://doi.org/10.1016/j.coastaleng.2017.10.004.

Schüttrumpf, H., 2001. Wave Overtopping Flow at Seadikes—Experimental and Theoretical Investigations (In German: Wellenüberlaufströmung bei Seedeichen—Experimentelle und Theoretische Untersuchungen). Ph.D. Thesis. Technische Universität Braunschweig, Braunschweig, Germany, 2001.

Schüttrumpf, H., Van Gent, M.R.A., 2003. Wave overtopping at seadikes. In: Proc. Coastal Structures Conference 2003, Portland, Oregon. ASCE, pp. 26–30.

Sigurdarson, S., van der Meer, J.W., 2012. Wave overtopping at berm breakwaters in line with Eurotop. In: Proc. ICCE 2012, Santander.

TAW, 2002. Technical Report Wave Run-Up and Wave Overtopping at Dikes, Technical Advisory Committee on Flood Defence. TAW, 2002.

Van Bergeijk, V., Warmink, J.J., Van Gent, M.R.A., Hulscher, S.J.M.H., 2019. An analytical model of wave overtopping flow velocities on dike crests and landward slopes. Coast Eng. 149, 28–38. https://doi.org/10.1016/j.coastaleng.2019.03.001.

Van der Werf, I.M., Van Gent, M.R.A., 2018. Wave overtopping over coastal structures with oblique wind and swell waves. J. Mar. Sci. Eng. 6 (4), 149. https://doi.org/10.3390/jmse6040149, 2018.

Van Doorslaer, K., 2018. Reduction of Wave Overtopping by and Wave-Induced Forces on Storm Walls and Promenades at Crest Level of Smooth Dikes; an Experimental Study. Ph.D. Thesis. Universiteit Gent, Belgium.

Van Gent, M.R.A., 1999. Physical Model Investigations on Coastal Structures with Shallow Foreshores; 2D Model Tests with Single and Double-Peaked Wave Energy Spectra, Delft Hydraulics Report H3608, December 1999, Delft.

Van Gent, M.R.A., 2001. Wave run-up on dikes with shallow foreshores. J. Waterw. Port, Coast. Ocean Eng. 127 (No.5), 254–262. Sept/Oct 2001.

Van Gent, M.R.A., 2002a. Coastal flooding initiated by wave overtopping at sea defences, ASCE, Proc. Coast. Disasters 2002, 223–237. San Diego.

Van Gent, M.R.A., 2002b. Wave overtopping at dikes, world scientific. Proc. ICCE 2002 vol. 2, 2203–2215.

Van Gent, M.R.A., 2019. Climate Adaptation of Coastal Structures, Keynote in Proc. Applied Coastal Research (SCACR 2019), Bari, Italy.

Van Gent, M.R.A., van den Boogaard, H.F.P., Pozueta, B., Medina, J.R., 2007. Neural network modelling of wave overtopping at coastal structures. Coast Eng. 54, 586–593.

Van Gent, M.R.A., 2020. Influence of oblique wave attack on wave overtopping at smooth and rough dikes with a berm. Coast Eng. 160 https://doi.org/10.1016/j.coastaleng.2020.103734.

Van Gent, M.R.A., 2021. Influence of oblique wave attack on wave overtopping at caisson breakwaters with sea and swell conditions. Coast Eng. 164 https://doi.org/10.1016/j.coastaleng.2020.103834.

Van Gent, M.R.A., Van der Werf, I.M., 2019. Influence of oblique wave attack on wave overtopping and wave forces on rubble mound breakwater crest walls. Coast Eng. 151, 78–96. https://doi.org/10.1016/j.coastaleng.2019.04.001.

Wolters, G., Van Gent, M.R.A., 2007. Maximum wind effect on wave overtopping of sloped coastal structures with crest elements. In: Proc. Coastal Structures 2007, Venice. World Scientific, pp. 1263–1274. https://doi.org/10.1142/9789814282024_0111.

Zelt, J.A., Skjelbreia, J.E., 1992. Estimating incident waves and reflected wave fields using an arbitrary number of wave gauges. In: Proc. ICCE 1992, Venice. https://doi.org/10.9753/icce.v23.%25p.

Glossary

α : slope angle of the structure [°]

β : angle of wave attack [°]

γ : influence factor [−]

γ_β : influence factor for the angle of wave attack [−]

γ_b : influence factor for a berm [−]

γ_f : influence factor for roughness [−]

γ_v : influence factor for a crest element [−]

$\xi_{m-1,0}$: surf-similarity parameter / Iribarren parameter based on H_{m0} and $T_{m-1,0}$ [-]

A_c : crest level of the armour at the crest [m]

B : berm width in the seaward slope [m]

B_L : berm level measured from the level of the armour at the crest to the berm level [m]

G_c : width of the armour at the crest in front of the crest wall [m]

g : acceleration due to gravity [m/s²]

H_{m0} : significant wave height of the incident waves based on the wave energy spectrum [m]

h : water depth [m]

h_b : berm depth with respect to the still water level (negative for emerged berm) [m]

$L_{m-1,0}$: wave length based on $T_{m-1,0}$ ($L_{m-1,0} = 2\pi /gT_{m-1,0}^2$) [m]

N : number of waves [−]

Q : non-dimensional mean overtopping discharge [−]

q : mean overtopping discharge [m³/s/m]

R_c : freeboard (crest height relative to the still water level [m]

$s_{m-1,0}$: wave steepness based on the wave height H_{m0} and the spectral wave period $T_{m-1,0}$ [-]

$T_{m-1,0}$: spectral mean wave period based on the ratio of the spectral moments m_{-1} and m_0 of the incident wave spectrum [s]